NJC

Accepted Manuscript

This article can be cited before page numbers have been issued, to do this please use: P. Jana, N. Patel, T. Mukherjee, V. Soppina and S. Kanvah, *New J. Chem.*, 2019, DOI: 10.1039/C9NJ01972C.

ROYAL SOCIETY OF CHEMISTRY

rsc.li/njc

View Article Online
DOI: 10.1039/C9NJ01972C

A "Turn-On" Michler's Ketone-Benzimidazole Fluorescent Probe for Selective Detection of Serum Albumins

Palash Jana[†], Nishaben Patel[‡], Tarushyam Mukherjee[†], Virupakshi Soppina[‡] and Sriram Kanvah[†]*

[†]Department of Chemistry, Indian Institute of Technology Gandhinagar, Palaj, Gujarat 382355, E-mail: sriram@iitgn.ac.in, kanvah@gmail.com.

[‡]Department of Biological Engineering, Indian Institute of Technology Gandhinagar, Palaj, Gandhinagar 382355. E-mail: vsoppina@iitgn.ac.in

Abstract

Interaction of Michler's ketone-benzimidazole derivatives (MK-**1** and MK-**2**) with serum albumin proteins was examined by absorption, steady-state, time-resolved fluorescence, molecular docking and circular dichroism methods. In the presence of albumins, a remarkable increase in fluorescence intensity and the quantum yield along with dominant color response was observed for cationic derivative **1** while neutral derivative **2** showed a weaker effect. The studies reveal synergistic effects of electrostatic, hydrophobic and H-bonding interactions in protein binding with the fluorophores. Competitive binding studies reveal selective binding of the probe to the albumin proteins over other commonly occurring analytes in the serum matrix. Bioimaging studies in HeLa cells showed the cytoplasmic distribution of the fluorophore with intense fluorescence signal. Serum depletion studies show a significant reduction in the fluorescence intensity that indicates binding affinity with albumins and their potential use for albumin detection.

Introduction

π-conjugated chromophores bearing electron donating (D) groups and electron withdrawing (A) groups have found extensive applications in organic electronics and biological applications[1-5]. The substitution of donor and acceptor moieties significantly influences the spectroscopic properties of the chromophores. In particular, amino donors such as N,N-dimethylaniline have been extensively used as a strong donor for linear and non-linear optical applications[6-8]. Michler's ketone (4,4′-dimethylamino benzophenone), is one such molecule bearing

View Article Online
DOI: 10.1039/C9NJ01972C

dimethylamine donating group and is widely used an intermediate in the production of dyes and pigments, such as crystal violet[9]. The favorable absorption in the UV region also enabled investigations into their photophysical and photochemical properties[10-14]. For most biological studies, it is preferable to have absorption and emission in the NIR region and appropriate chemical moieties to improve binding affinity. Taking cognizance of the need for red-emitting probes, over the years, researchers have developed several push-pull fluorophores for biological applications[15-21]. However, reports on push-pull derivatives based on the Michler's ketone scaffold are limited to their use as photoinitiators[22-24] or for chelation[25]. The optical properties of Michler's Ketone reveal an absorption maximum of 365 nm and emission about 500 nm[22], and there are no known reports of these strongly colored derivatives for potential biological use. Considering the favorable optical properties of Michler's ketone derivatives, herein we report utilization of this scaffold for probing the small molecule-protein interactions. To induce favorable protein or biomolecule interactions, we introduced a biologically active moiety, benzimidazole, as a substituent. Benzimidazoles are part of many drug molecules exhibiting anti-bacterial, anti-fungicidal, anti-helminthic and anti-cancer applications[26-30] and known to bind with microtubules stopping hyphal growth in fungi or blocking nuclear division[31-34]. Furthermore, benzimidazole derivatives are also structural units in several molecular systems that have organic electronic or sensing applications[35-39]. Taking cognizance of these two scaffolds (Michler's Ketone and benzimidazole), we report the synthesis of neutral and cationic fluorophores [Scheme-1] and investigated the absorption and emission in various solvents. We further probed the protein-ligand interactions involving serum albumins. The molecules show emission greater than 600 nm and exhibit strong selective emission enhancement in the presence of serum albumins. Bioimaging studies indicate the cytoplasmic distribution of the fluorophore. The results (absorption, fluorescence, lifetime studies and binding investigations in the presence of serum albumins and cellular imaging) are detailed below.

Experimental

All the chemicals, reagents required for the synthesis of the benzimidazole derivatives and spectroscopic studies were purchased from Sigma-Aldrich, Alfa Aesar, Acros and S. D. FineChem and were used as such. All the synthesized samples were characterized using ^{1}H NMR and ^{13}C NMR in $CDCl_3$ or DMSO-D_6 using Bruker Avance III-500 MHz NMR spectrometer.

View Article Online
DOI: 10.1039/C9NJ01972C

Mass spectral data were obtained using ESI-QToF Waters- Synapt G2S High-resolution mass spectrometer. UV-Vis absorption spectra were recorded using Analytik Jena specord 210 plus and the fluorescence emission studies were performed using Horiba-Jobin-Yvon Fluolorog-3 spectrofluorimeter. Typically, the excitation wavelengths were set at the absorption maxima (λ_{abs}) of the compounds under investigation. All the fluorescence spectra were recorded in 10 mm path length quartz cuvette with a slit width of 2 nm. Fluorescence quantum yields of compounds were estimated using cresyl violet (Φ = 0.56 in EtOH) as a reference standard[40]. For the fluorescence measurements, ~10 μM concentrations of chromophores were used. Circular dichroism (CD) spectra were carried out at room temperature on a Jasco J-815 spectropolarimeter. The fluorescence lifetime measurements were performed using a picosecond time-correlated single photon counting (TCSPC) setup (Edinburgh instrument Ltd, Life spec II model) employing a picosecond light emitting diode laser at 515 nm for the excitation of the neutral form of the dye and dye-albumin complex. A reconvolution procedure was used to analyze the decay by using a proper instrument response function (IRF) obtained by using LUDOX, HS-40 colloidal silica particles in a 40 wt% suspension in water as the light scatterer. The fluorescence decays [$I(t)$] were analyzed in general as a sum of exponentials eqn.(1)

$$I(t) = \sum B_i \exp(-t/\tau_i) \qquad (1)$$

where B_i and τ_i are the pre-exponential factors and fluorescence lifetime of the ith component. Reduced chi-square (χ^2) values and the random distribution of the weighted residuals among data channels were used to judge the acceptance of the fits. The percent error associated with the lifetime studies is 0.30–13%. K_{nr} has been calculated through following eqn.(2)

$$K_{nr} = (1-\Phi)/\tau \qquad (2)$$

Albumin binding studies with dyes were conducted in phosphate buffer solution. The desired compounds were prepared as per the synthetic methodology is given in Scheme-1. In a typical procedure, the synthesis of Michler's Ketone derivatives was achieved through synthetic scheme-1 given below. First, the keto group of Michler's derivative **5** is converted to olefin **4** through a Wittig reaction in the presence of methyltriphenylphosphonium bromide. Formyl product **3**is achieved through a Vilsmeier-Haack reaction. Condensation of aldehyde **3** with

View Article Online
DOI: 10.1039/C9NJ01972C

nitrile derivative of benzimidazole yields MK-**2** which on methylation with methyl iodide yields cationic derivative **1**.

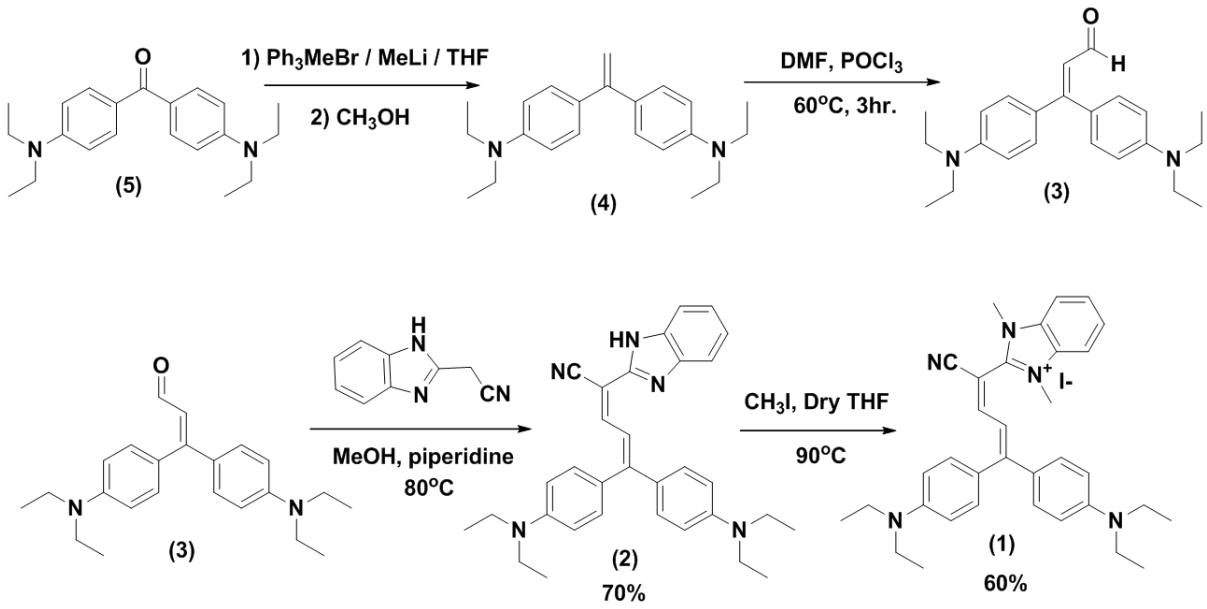

Scheme-1: Synthetic scheme for the preparation of the benzimidazole derivatives of Michler's Ketone.

Synthesis of MK-2

Compound **3** was obtained through previously published literature[41]. Compound **3** [0.807 mmol, 1equiv] and 2-benzoimidazolyl acetonitrile [1.2 mmol, 1.5equiv] and 0.5mmol of piperidine were mixed in 20mL anhydrous methanol. The mixture was refluxed at 110°C for 5h and the reaction was monitored by thin layer chromatography (TLC) until the consumption of the aldehyde. Upon completion, the contents of the reaction were cooled to room temperature, the solvent was evaporated and the residue was washed with diethylether and hexane. 30ml of diethyl ether was added to the residue, the precipitate obtained was filtered and dried under vacuum for 1h to afforded MK-**2** as a red solid (170 mg, 0.751mmol). Yield:70%

2-(1H-Benzoimidazol-2-yl)-5,5-bis-(4-diethylamino-phenyl)-penta-2,4-dienenitrile(**2**):Yield 70%(150mg): ^{1}HNMR (500MHz, $CDCl_3$) δ (ppm): 9.43(s,1H), 8.12-8.10(d, *J*=10 Hz,1H), 7.66-7.64(t, *J*=5Hz,1H), 7.38-7.35(t, *J*=5Hz,1H), 7.35-7.33(d, *J*=10Hz, 2H) 7.22-7.20(q, *J*=5Hz,2H), 7.12-7.10(d, *J*=10Hz,2H), 7.07-7.04(d, *J*=10Hz,1H), 6.65-6.61(q, *J*=5Hz, 4H) 3.44-3.399

View Article Online
DOI: 10.1039/C9NJ01972C

(m,8H), 1.24-1.19 (m,12).^{13}C-NMR (125MHz, $CDCl_3$): δ (ppm)158.48, 149.17, 148.72, 148.05, 146.98, 144.21, 133.13, 132.90, 131.39, 127.89, 125.12, 123.15, 122.72, 119.12, 118.10, 117.48, 110.92, 110.78, 110.46, 96.22, 44.49, 44.36, 12.76, 12.765 HRMS (ESI-Q-TOF): $C_{32}H_{35}N_5$ $[M+H]^+$: cal. m/z 490.2965 , found, 490. 2940 m/z.

Synthesis of MK-1

In a 25 mL round bottomed flask, MK-**2** [0.40mmol, 1equiv] in 15ml of dry THF was added followed by the addition of 10 equiv. of methyl iodide. The mixture was refluxed at 90°C for 24h. After completion of the reaction the solvent was evaporated and the residue was washed with diethyl ether and hexane. Desired product was purified by column chromatography initially with 30% ethyl acetate/ hexane to remove the starting material and later with 5% MeOH/CH_2Cl_2. Evaporation of the solvent followed by drying affordedMK-**1** as a dark-red solid. (80mg 0.143mmol). Yield: 60%

2-[1-Cyano-4,4-bis-(4-diethylamino-phenyl)-buta-1,3-dienyl]-1,3-dimethyl-3H-benzoimidazol-1-ium iodide**1:** Yield 60% (80mg) ^{1}HNMR (500MHz, DMSO-d_6) δ (ppm): 8.02-8.00(q, *J*=2.5Hz, 2H), 7.69-7.67(q, *J*=2.5Hz,2H), 7.65-7.63(d, *J*=10Hz,1H) 7.38-7.36(d, *J*=10Hz,2H)7.25-7.23(d, *J*=10Hz, 2H) 7.01-6.98(d, *J*=10Hz,1H) 6.81-6.77(q, *J*=5Hz,4H) 4.01(s,1H), 3.47-3.41(m, 8H), 1.17-1.13(m,12H)^{13}C-NMR (125MHz, DMSO-d_6): δ (ppm)164.17, 157.89, 150.69, 150.44, 149.84, 146.67, 134.02, 132.69, 132.37, 126.96, 126.13, 123.98, 1115.76, 115.53, 113.94, 113.81, 111.78, 111.35, 111.11, 82.68, 44.42, 44.21, 33.46, 12.99, 12.97HRMS (ESI-Q-TOF): $C_{34}H_{40}N_5^+[M]^+$: cal. m/z 518.3278 , found, m/z 518.3269. NMR spectral data are given in Fig S13-S16.

Molecular Docking study:

Insilico docking studies were carried out using the Glide module (XP) of Schrödinger Maestro v11.3 software. The entire docking process was performed in the following steps: Protein preparation, receptor grid generation, ligand preparation and ligand docking. The desired crystal structure of the BSA protein was downloaded from the protein data bank (PDB ID: 4F5S). The protein was further prepared by the help of protein preparation wizard and water molecules were removed and polar hydrogens were added. Grid around the active site of the

View Article Online
DOI: 10.1039/C9NJ01972C

protein was generated by receptor grid generation module; and MK-**1** and MK-**2** molecules were drawn in 2D sketcher and the energy optimized structures were obtained by the help of LigPrep module. Thereafter the ligands were docked onto the specific site of BSA (Sudlow's site II) using the Glide docking ligands module of Schrodinger and the docked conformations were visualized and represented using the Maestro v11.3.

Cell culture and Imaging

HeLa cell line was a kind gift from Roop Mallik lab (TIFR, Mumbai). The cells were cultured in DMEM (Dulbecco's Modified Eagle Medium) supplemented with 10% FBS (fetal bovine serum) and 2mMGlutaMAX (Gibco) at 37°C with 5% CO_2. For fluorescence imaging, HeLa cells were seeded on coverslips at a cell density of $1.5x10^5$/well in a 6-well plate. The cells were then incubated with 1 μM probe in the culture medium for 60 min at 37°C in the CO_2 incubator. For serum depletion experiment, HeLa cells were seeded on coverslips at a cell density of $1.5x10^5$/well in a 6-well plate. The cells were then incubated with 1 μM probe in a cell culture medium for 60 min at 37°C in the CO_2 incubator. Next, the cells were washed with PBS and incubated with serum-free media for the following time-points: 0 h, 1 h, 2 h, and 3 h. Coverslips were fixed for each time-point. Before fixing, coverslips were rinsed three times with phosphate buffer solution (PBS), fixed in freshly prepared 4% PFA (paraformaldehyde) in PBS for 5 minutes, and quenched with 50 mM ammonium chloride in PBS for 5 min. The coverslips were mounted using Prolong Gold (Life Technologies). Images were obtained using the epi-fluorescence microscope (Nikon EclipseT*i*-U) equipped with DS-Qi1 camera (Nikon).

Data analysis

ImageJ software (nih.gov) was used for microscope image analysis and quantification. Cells were randomly selected to perform the quantification. Value of maximum/mean fluorescence intensity was obtained from ImageJ for the red filter. Background fluorescence was subtracted from this mean value. This fluorescence intensity values were plotted, and statistical analysis was performed using Origin software.

View Article Online
DOI: 10.1039/C9NJ01972C

Results and Discussion

Absorption and Emission

Two Michler's ketone derivatives were synthesized bearing a cationic (MK-**1**) and neutral benzimidazole (MK-**2**) moieties. The molecular unit bears a nitrile group on the double bond serving as an additional acceptor group along with benzimidazole moiety. The nitrile group on the double bond also restricts double bond rotation and may enable aggregation induced emission characteristics[42-44]. The presence of both electron donating (diethylamine) and acceptor (benzimidazole) moieties results in strong charge separation. The absorption and emission of the MK derivatives are shown in Fig-1. The cationic derivative (MK-1) has an absorption maximum at 530 nm in acetonitrile, while the neutral derivative (MK-2) shows an absorption maximum at 490 nm (Table-1). The bathochromic shifts in the absorption maxima are attributed to the improved electron acceptor strength of the cationic benzimidazole moiety. Solvent polarity variations do not affect the absorption maxima for both the MK derivatives indicating weak solvent stabilization[45]. The emission spectra of the MK-**1** and **2** are given in Fig2a and Fig2b. Similar to the absorption, bathochromic emission shifts were observed for the cationic derivative (~645-650 nm) over neutral derivative (emission maxima ~595 nm-600 nm). Solvent polarity dependent emission shifts were not observed despite having strong donor and acceptor groups. This is due to the greater flexibility of the molecule hindering the formation of strong charge separated states and subsequent weaker solvent stability of the excited state species. The quantum yields of emission with respect to cresyl violet were calculated for (MK-1) and are found to be low (0.00147) revealing strong non-radiative energy losses due to bond-rotations and competitive electron transfer to nitrile and benzimidazole groups.

View Article Online
DOI: 10.1039/C9NJ01972C

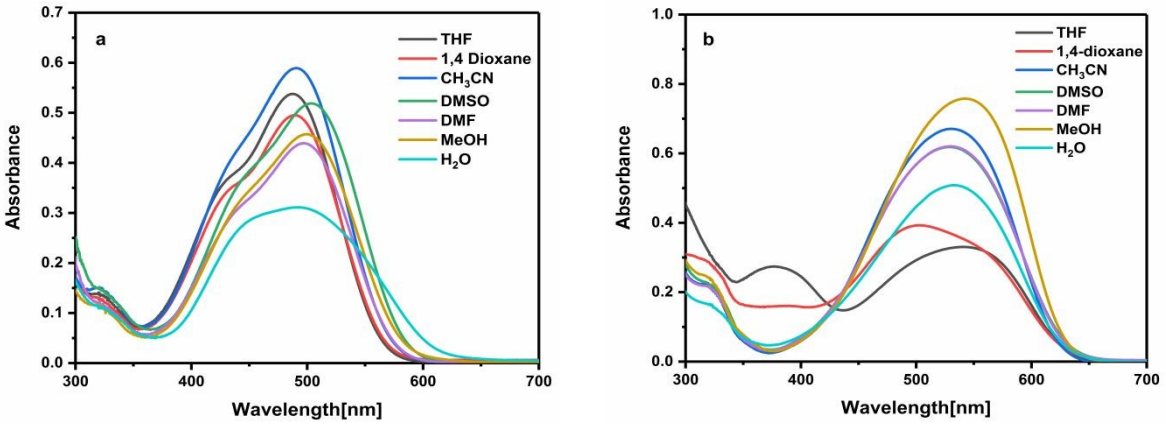

Fig.1 Absorption spectra of a) MK-**2** and b) MK-**1** in solvents of varying polarity

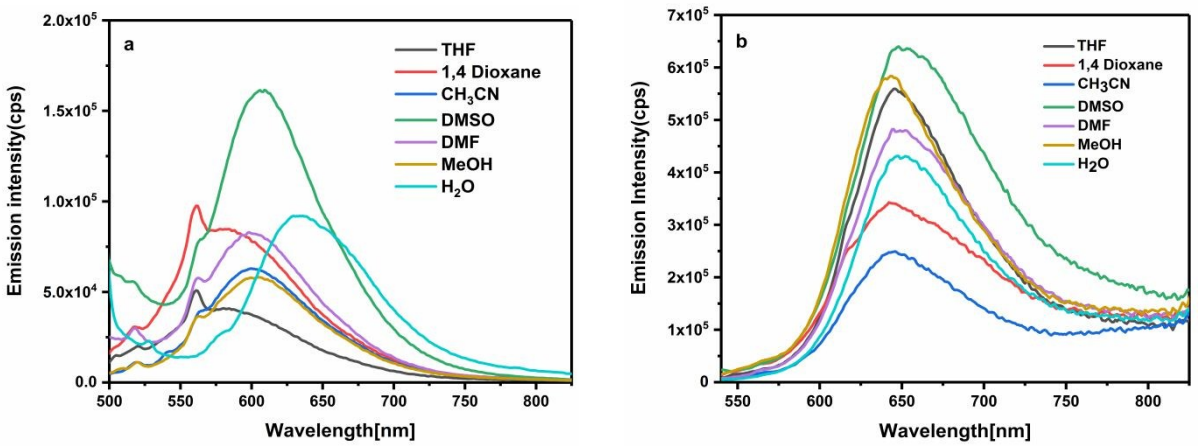

Fig.2 Emission spectra of a) MK-**2** and b) MK-**1** in solvents of varying polarity. Excitation wavelength used is 490 for MK-**2** and 530 nm for MK-**1.**

Table-1: Absorption and emission data of Michler's Ketone derivatives **1** and **2** in solvents.

	MK-1		**MK-2**	
Solvent	λ_{abs}(nm)	λ_{em}(nm)	λ_{abs}(nm)	λ_{em}(nm)
THF	538	645	488	581
1,4-dioxane	501	643	490	580
CH_3CN	530	644	490	600
DMSO	532	650	504	607
DMF	530	648	498	600
MeOH	543	643	500	604
H_2O	534	650	493	632

View Article Online
DOI: 10.1039/C9NJ01972C

Binding with Albumins

While the compounds are weakly fluorescent, we hypothesized that the favorable absorption and emission behavior could be immensely useful in investigating the biomolecular interactions. For this, we have chosen serum albumins (Bovine serum albumin (BSA) and Human serum albumin (HSA), common transport proteins that are abundantly found in the bloodstream with remarkable binding ability[17, 46, 47]. In the presence of the albumin proteins, MK-1 shows a moderate red-shift (~18 nm) in the absorption maxima, revealing the interaction of the chromophore with the protein [Fig-3a]. Titration of the chromophore with albumin yields significant emission intensity enhancement (~78 fold) along with enhanced quantum yields (from 0.0014 to 0.093, 66 folds) [Fig 3b] indicating favorable binding of the probe with albumin proteins. The observations with HSA are similar with ~60 fold emission intensity enhancement (Fig.S1). On the other hand, the neutral derivative MK-2 shows little effects on the absorption maxima (Fig S2a and S3a). The emission maxima show a small hypsochromic shift (5-10 nm) with weak intensity enhancement (~1.5 fold increments) [Fig. S2b & Fig.S3b]. The hypsochromic emission shifts reveal potential interaction of the fluorophore with the hydrophobic domains of the protein matrix. These observations further reiterate strong interactions of the cationic group in MK-1, resulting in enhanced emission signal for MK-1 with proteins. Distinct visual colors were also noted upon addition of albumin [inset: Fig 3a]. To evaluate the general utility of identifying the albumin content, a strip test was also performed for HSA & BSA in 200μM concentration [Fig. S4] revealing color changes in the presence of the albumin.

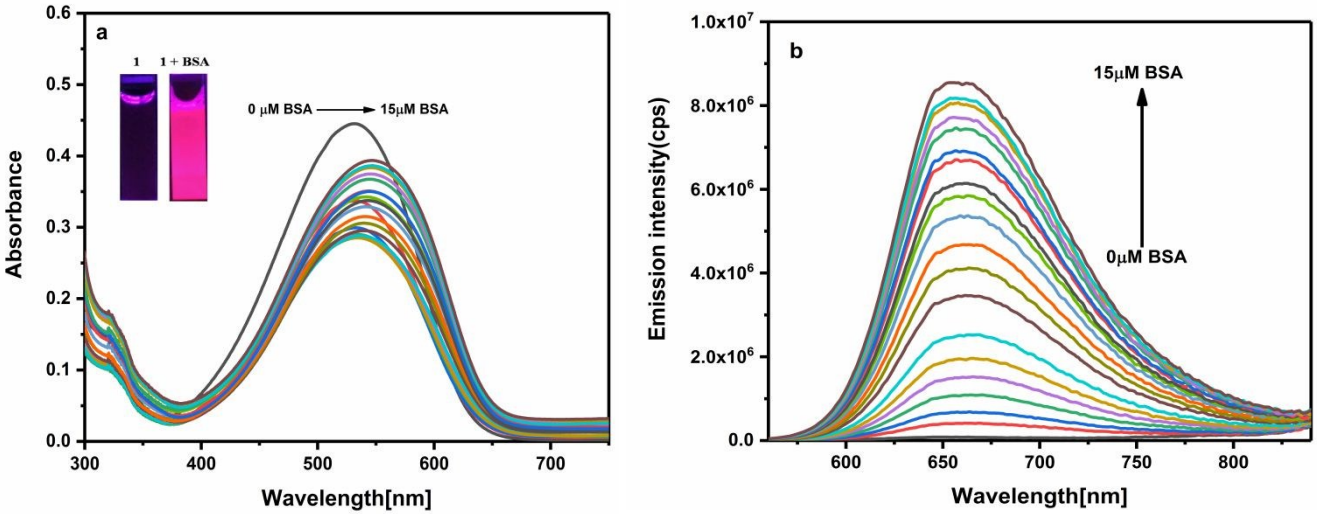

View Article Online
DOI: 10.1039/C9NJ01972C

Fig. 3a) Absorption spectra and (b) fluorescence spectra of an ensemble of MK-**1** (10 μM) in PBS buffer (10mM) solution after the addition of different amounts of BSA from 0–15μM. $\lambda_{ex.}$ =540nm, Each solution was mixed and left for 1 min before recording the spectra. Inset: MK-**1** without BSA and (MK-**1**+BSA) seen under a UV lamp (365 nm).

Fluorescence lifetime measurements

To support the investigations, fluorescence decay experiments were measured. In aqueous PBS buffer solution, fluorophore MK-**1** shows a lifetime of 0.54ns due to its non-fluorescent nature. However, after the addition of 15μM BSA to the dye solution (10 μM) in 10mM PBS buffer, the decay times became slower (Fig.4). The average excited state lifetime of MK-**1** in the presence of BSA was calculated to be 1.24ns. In the case of HSA, similar observations were noted with excited state lifetime of 1.19ns as shown in Table-2. This increase of the lifetime value in the presence of BSA and HSA and suggests binding of the MK-**1** to BSA or HSA. The binding of the ligand with the proteins result in changes to non-radiative decay rates from = 1.84 ns^{-1} in the buffer solution to K_{nr} =0.731 ns^{-1}, K_{nr} = 0.783 ns^{-1}in the presence of BSA and HSA respectively.

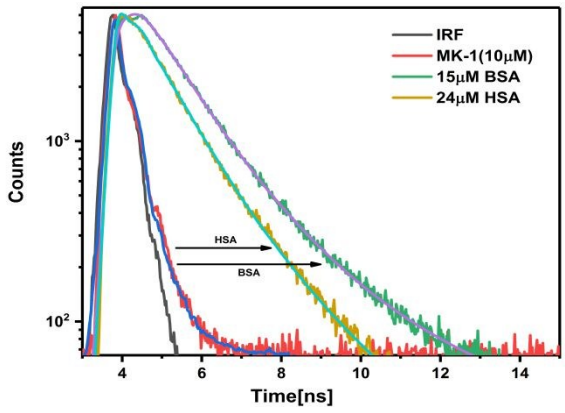

Fig.4 Lifetime decay profile of MK-**1** in PBS buffer solution with BSA & HSA at 515 nm excitation.

View Article Online
DOI: 10.1039/C9NJ01972C

Table 2 Average lifetime data of **MK-1** in the presence of BSA and HSA.

Component	τ_1 (ns)	B1(%)	τ_2(ns)	B2(%)	τ_3(ns)	B3(%)	<τ>(ns)	χ^2
MK-**1**	0.01	93.71	1.07	6.29	-	-	0.54	1.2
MK-**1**+ BSA	0.09	16.79	1.03	64.75	2.6	(18.46)	1.24	1.3
MK-**1**+ HSA	0.1	19.72	0.98	62.32	2.49	(17.96)	1.19	1.2

CD measurements

To investigate the conformational changes of serum albumin upon dye binding, we performed circular dichroism measurements. Native protein (BSA) exhibits two negative peaks at 222 nm and 208nm respectively[48] as depicted in Fig-5. The negative peaks increase drastically from 208nm to 225nm with the addition of MK-**1** & MK-**2**. The loss of the 208 nm CD band (Fig. 5) reveals that upon the interaction of the probes, structures of BSA and HSA are modified drastically. Similar results were obtained with HSA. From the CD observations, it is clear that both the dyes interact with albumin effectively inducing strong conformational changes[18]. However, fluorescence intensity changes of MK-**1** are more dramatic than for MK-**2** and this could be due to the presence of additional binding forces from the positively charged groups.

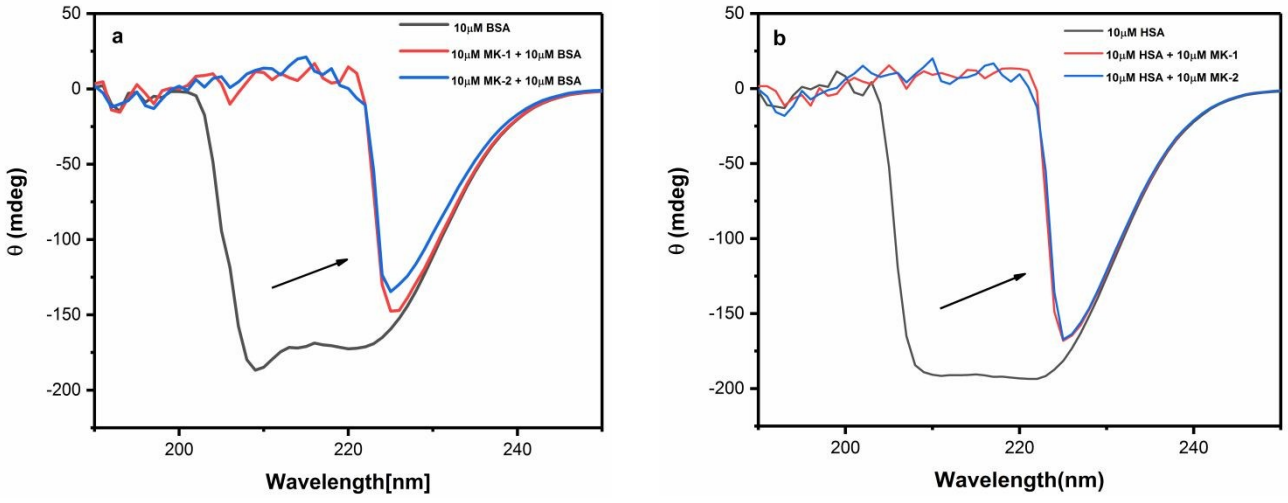

Fig.5 CD spectra of a) BSA b) HSA with the presence of MK-**1** & MK-**2** in PBS buffer (10mM, pH 7.4) at 298K

View Article Online
DOI: 10.1039/C9NJ01972C

Binding Site Determination

Albumins contain three α-helical domains I, II, III that are further divided into two subdomains A & B. The two major binding sites are located within sub domain IIA and IIIA sometimes referred to as Sudlow site I (Warfarin binding sites) and II (Ibuprofen binding site) respectively[16, 49]. Hydrophobic interactions are a dominant operative force for the site-I while interactions within site-II involved H-bonding, electrostatic interaction, van der Waals forces, and hydrophobic forces. Both the cavities play an important role in drug development, especially in pharmacokinetics and pharmacodynamics[25, 50, 51]. Binding of the fluorophore to the protein can directly influence the fluorescence of the protein and the fluorophore through its interaction with the protein microenvironment and accessibility to the solvent. Such interaction can result in emission quenching or enhancement apart from hypsochromic or bathochromic emission shifts. MK-1 is essentially non-fluorescent in aqueous media and the binding of the fluorophore to the albumin yields strong color and enhanced emission intensity indicating a strong interaction of the dye with albumin binding pockets. Titration of the dye with BSA yields a binding constant of 2.68 x $10^5 M^{-1}$ suggesting good binding affinity of the fluorophore with BSA with a 1:1 binding fit [Fig.S5]. The limit of detection for BSA was found to be 816 nM [Fig.S6]. In the case of HSA,the experimental data also supports a 1:1 binding model with a measured binding constant of 3.07 x 10^4 M^{-1} [Fig. S7] with the detection limit of 1.30μM [Fig.S8].

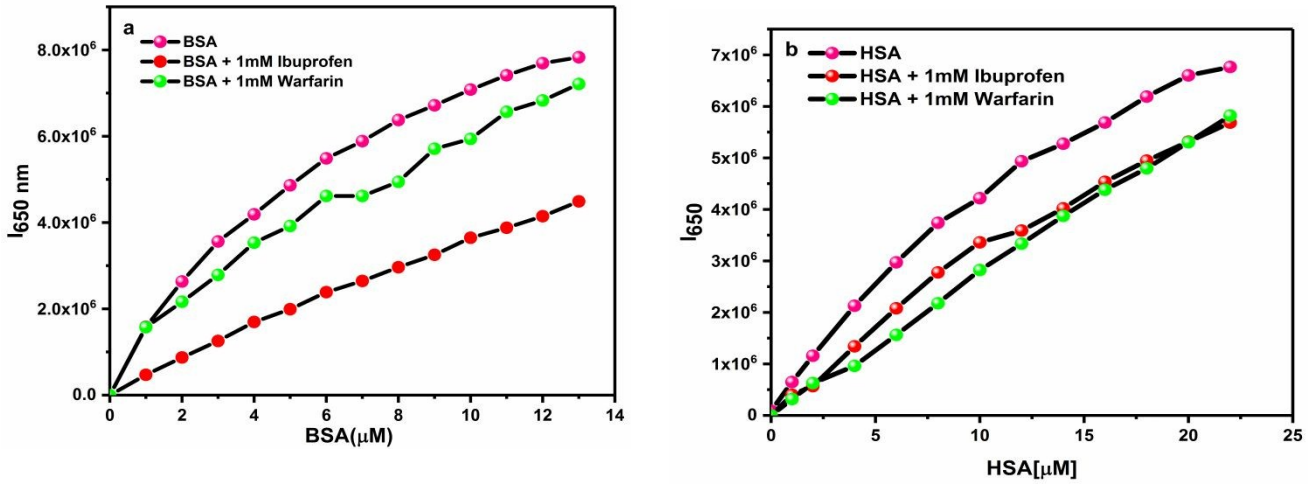

Fig. 6 Competitive binding plot of ibuprofen and warfarin in the presence of a) BSA b) HSA in PBS buffer solution.

View Article Online
DOI: 10.1039/C9NJ01972C

Competitive Assay and Selectivity

Competitive binding experiments with ibuprofen and warfarin were also performed to understand the nature of the binding interaction of MK-1 with albumin proteins. For this experiment, we mixed dye (MK-1) solution, 1mM solution of warfarin or ibuprofen and titrated with different concentration of serum albumins. In the case of BSA, ibuprofen showed a greater reduction (47% displacement of the ligand) of fluorescence intensity as compared to warfarin (13% displacement) [Fig. 6 and Fig.S9]. The observed results suggest that MK-1 predominantly bind to Sudlow's site-II of BSA. Increased addition of ibuprofen displaces the fluorophore from its binding domain resulting in the emission losses. In the case of HSA, the fluorescence intensity of MK-1 shows a smaller reduction (around 15% displacement) suggesting that MK-1 may interact equally with both the binding sites [Fig.S10].

One of the important criteria for the practical use of the probes is selectivity. For evaluation of the selectivity toward BSA and HSA, we tested different biological analytes (Lysozyme, trypsin, hemoglobin) along with amino acids (aspartic acid, lysine, and cysteine) and inorganic salts (NaCl, KCl, $CaCl_2$), the common constituents of the serum albumin. The results summarized in the Fig.7 show largest emission response for BSA and HSA while the response with other interfering analytes is insignificant. Competitive emission binding studies of MK-1 in the presence of BSA and HSA with other analytes [Fig.S11] reveal its affinity for albumins.

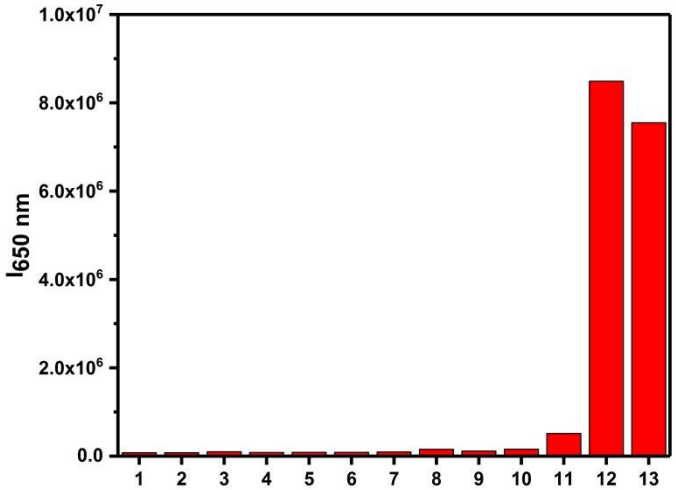

Fig.7 Histogram of MK-1at 645nm in PBS buffer solution (10mM, pH = 7.4, containing 1% DMSO) with various analytes. 1) dye alone 2) Aspartic acid (0.5M), 3) Lysine (0.5M) 4) Cysteine (0.5M) 5) KCl (0.5M), 6) NaCl (0.5) 7) $CaCl_2$ (0.5M) 8) Lysozyme (15µM) 9) Trypsin (15µM) 10) Catalase (15µM) 11) Hemoglobin(15µM) 12) BSA(15µM) 13) HSA (15µM)

View Article Online
DOI: 10.1039/C9NJ01972C

Docking Study

To better understand the fluorophore-protein interactions and the ensuing emission response, we performed *in silico* docking study for MK-**1** & MK-**2** with BSA. MK-**1** interacts with Arg409 of the BSA protein through π-cation with a docking score -3.3 Kcal mol^{-1} (Fig 8). However, MK-**2** shows H- bonding with Gln389 and π-cation interactions with Arg409 amino acid involving dock score of -3.6 Kcal mol^{-1}. Apart from revealing the information regarding the interacting amino acids, it demonstrates that benzimidazole moieties of MK-**1** and MK-**2** were exposed to solvent and two N,N-diethyl phenyl groups of MK-**1** were located at site-II amino acid pocket, which in turn, may restrict the single bond rotation of N,N-diethyl groups [Fig.8C&D] and consequently contributing to the enhanced emission intensity. On the other hand, in MK-**2**, one donor group was located in the amino acid pocket, and another was exposed to the surrounding solvent environment, giving rise to a twisted conformation in the binding site of BSA [Fig.8A&B] resulting in weaker emission response. We expect similar kind of interaction with HSA due to the structural similarity of HSA with BSA.

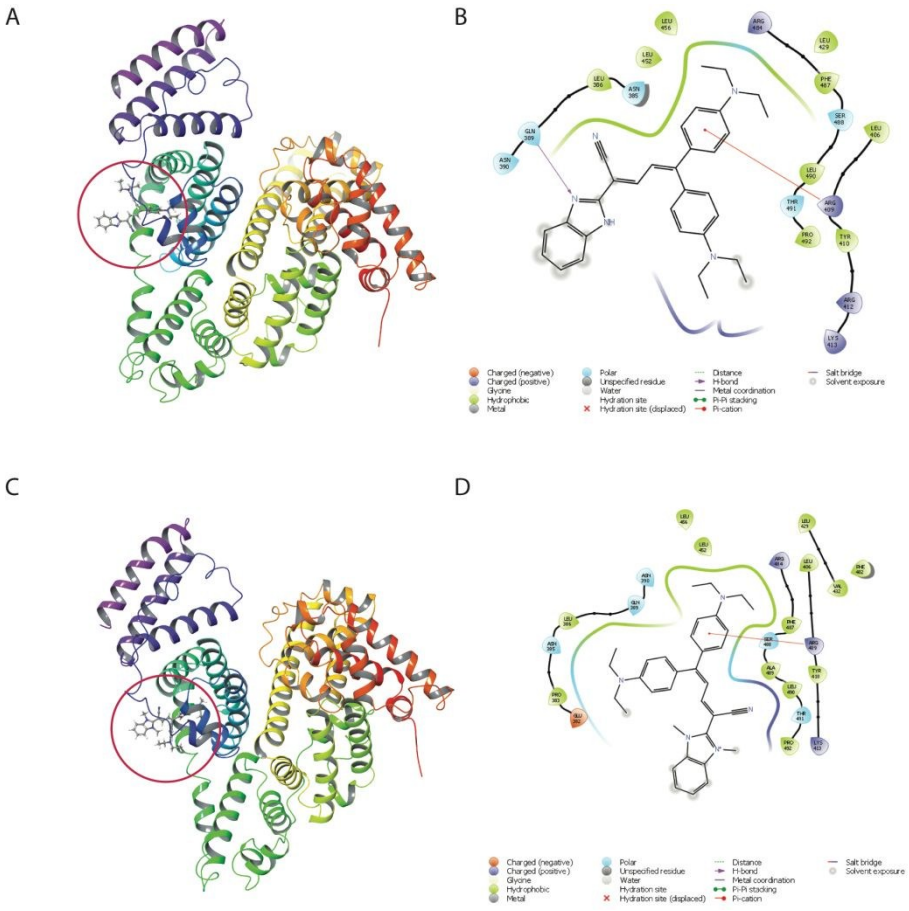

View Article Online
DOI: 10.1039/C9NJ01972C

Fig.8 Molecular Docking models; Best docking conformation and the interaction diagram of MK-**2**[(A) and (B) respectively], MK-**1**[(C) and (D) respectively] with BSA protein.

Cellular imaging

Upon treatment of HeLa cells with 1 μM MK-**1**, we observed intense red fluorescence (Fig. 8). However, the dye showed the uniform cytoplasmic distribution and did not show any specific subcellular localization. The MK-**1** concentration used (1 μM) for bioimaging studies showed negligible cell death. Notably, no significant cell death (30%) was observed even when cells were treated with 10 μM MK-**1** [Fig.S12]. Remarkably, MK-**1** showed higher specificity to serum albumins, a major component for cell growth. Therefore, we decided to further explore MK-**1** under serum-free conditions (Fig.9) in a time-dependent manner (0h, 1h, 2h, and 3h). Interestingly, a significant decrease in fluorescence intensity was observed within an hour of serum depletion (Fig.9). However, no further decrease in the fluorescent intensity was observed in subsequent time points. Taken together, our data indicate that MK-**1** has higher specificity for serum albumin. This study highlights the possibility of using Michler's Ketone scaffold as an efficient fluorescence probe for detection and monitoring of albumins.

View Article Online
DOI: 10.1039/C9NJ01972C

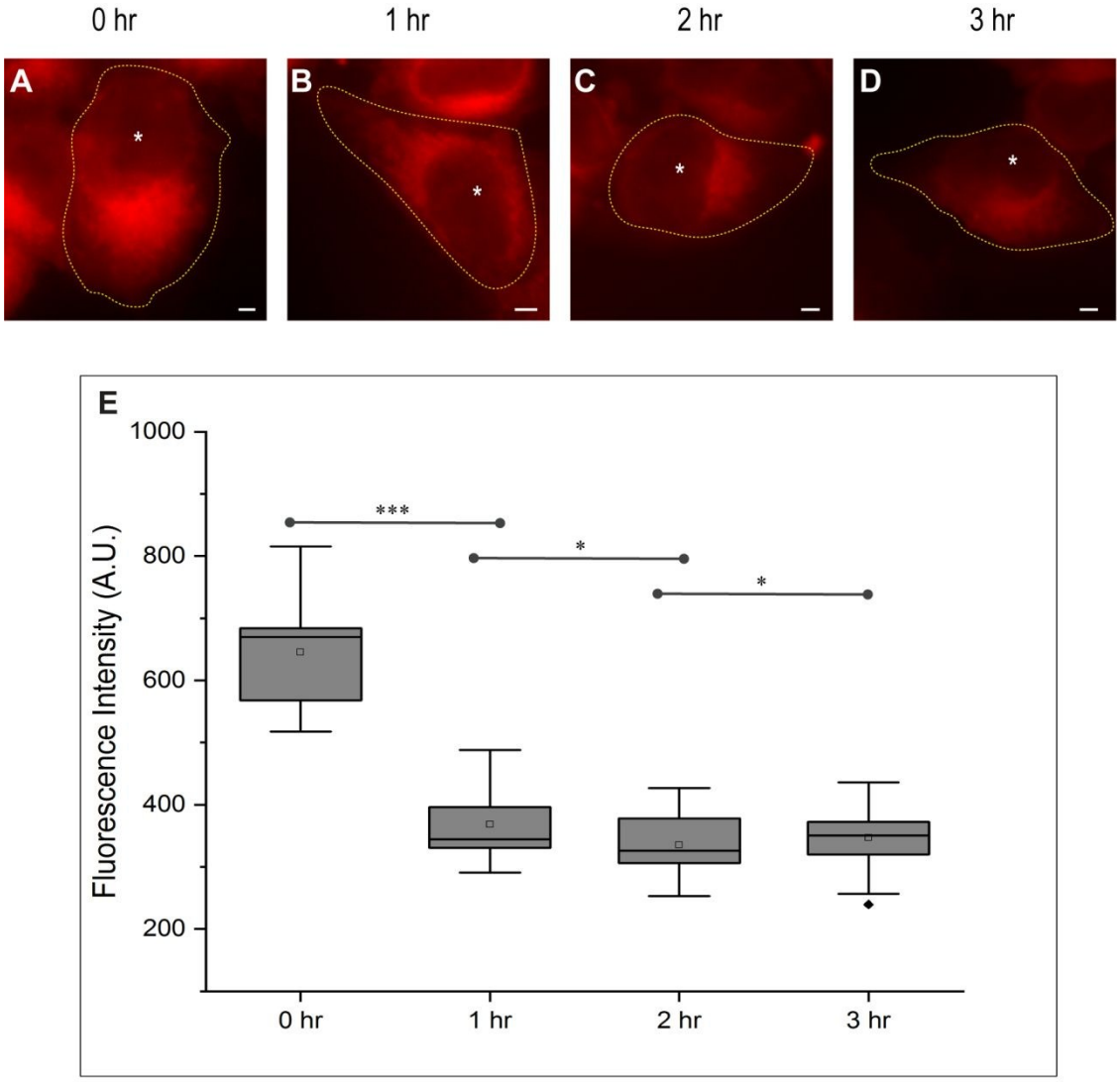

Fig.9 Serum depletion leads to a decrease in MK-**1** fluorescence**.** Fluorescence images of HeLa cells incubated with MK-**1** at 1 μM concentration for 60 min, followed by serum depletion for 0h, 1h, 2h, and 3h (A-D). Excitation at 561 nm for the red channel (630-720 nm). Quantification of fluorescence intensity for each time-point (E). Yellow dashed line – Cell boundary; Asterisk - Nucleus; Scale bar – 10 μm. n = 11-15 cells for quantification. *P* values were calculated using two-sample t-test: ****p<0.005, **p<0.05, *p<0.5.*

View Article Online
DOI: 10.1039/C9NJ01972C

Conclusions

In conclusion, we synthesized neutral and cationic π-conjugated Michler-benzimidazole derivatives with absorption and emission in the visible regions. Furthermore, MK-1 is highly selective towards the recognition of serum albumin even in the complex sample media containing various interfering biomolecular analytes. The drug displacement study reveal possible propensity of the dye towards domain IIIA (Sudlow site II) in case of BSA and spread out in both domain sites of HSA. Cellular imaging studies with HeLa cells demonstrate cytoplasmic distribution and decreased fluorescence in the absence of serum indicate affinity of the dye to albumin. Overall, the remarkable properties of MK-1 could be beneficial as a practical probe for various molecular biology and biomedical applications.

Supporting Information

Additional figures and spectral characterization data (Fig S13-S16) are provided

Acknowledgments

SK acknowledges a financial grant from BRNS (Board of Research in Nuclear Sciences), India; 37(2)/14/05/2016). VS acknowledges DBT (Grant No: BT/PR15214/BRB/10/1449/2015 and BT/RLF/Re-entry/45/2015) and DST-SERB (Grant No: ECR/2016/000913) for financial support. PJ, NP, TM acknowledge IIT Gandhinagar for their fellowship. General infrastructural support from IIT Gandhinagar acknowledged.

References

1. R. Sen, S. P. Singh and P. Johari, *J. Phys.Chem. A*, 2018, **122**, 492-504.
2. A. S. Klymchenko, *Acc. Chem. Res.*, 2017, **50**, 366-375.
3. Y. Li, T. Liu, H. Liu, M.-Z. Tian and Y. Li, *Acc. Chem. Res.*, 2014, **47**, 1186-1198.
4. W. Zhang, J. Yao and Y. S. Zhao, *Acc. Chem. Res.*, 2016, **49**, 1691-1700.
5. D. Li, W. Hu, J. Wang, Q. Zhang, X.-M. Cao, X. Ma and H. Tian, *Chem. Sci.*, 2018, **9**, 5709-5715.
6. B. J. Coe, J. A. Harris, I. Asselberghs, K. Wostyn, K. Clays, A. Persoons, B. S. Brunschwig, S. J. Coles, T. Gelbrich and M. E. Light, *Adv. Funct. Mater.*, 2003, **13**, 347-357.
7. B. Ruiz, Z. Yang, V. Gramlich, M. Jazbinsek and P. Günter, *J. Mater. Chem.*, 2006, **16**, 2839-2842.
8. H. Agnihotri, A. K. Vasu, V. Palakollu and S. Kanvah, *Photochem. Photobiol. Sci.*, 2015, **14**, 2159-2167.
9. A. Noack, A. Schröder and H. Hartmann, *Angew.Chem.Int. Ed.*, 2001, **40**, 3008-3011.
10. Y. Fujita, K. Higuchi, H. Nishikiori, N. Tanaka and T. Fujii, *J. Photochem. Photobiol. A: Chem.*, 2006, **179**, 156-160.
11. J. A. Mondal, H. N. Ghosh, T. K. Ghanty, T. Mukherjee and D. K. Palit, *J. Phys.Chem. A*, 2006, **110**, 3432-3446.

View Article Online
DOI: 10.1039/C9NJ01972C

12. Y.-P. Zhao, L.-Y. Yang and R. S. H. Liu, *Green Chem.*, 2009, **11**, 837-842.
13. M. V. Barnabas, A. D. Liu, A. D. Trifunac, V. V. Krongauz and C. T. Chang, *J. Phys. Chem.*, 1992, **96**, 212-217.
14. D. I. Schuster, M. D. Goldstein and P. Bane, *J. Am. Chem. Soc.*, 1977, **99**, 187-193.
15. K. Rajasekhar, C. J. Achar and T. Govindaraju, *Org. Biomol. Chem.*, 2017, **15**, 1584-1588.
16. G. Chakraborty, A. K. Ray, P. K. Singh and H. Pal, *Chem.Commun.*, 2018, **54**, 8383-8386.
17. V. S. Jisha, K. T. Arun, M. Hariharan and D. Ramaiah, *J. Phys.Chem. B*, 2010, **114**, 5912-5919.
18. V. S. Jisha, K. T. Arun, M. Hariharan and D. Ramaiah, *J.Am.Chem. Soc.*, 2006, **128**, 6024-6025.
19. N. Barbero, C. Butnarasu, S. Visentin and C. Barolo, *Chem. Asian J.*, 2019, **0**.
20. N. Johnsson and K. Johnsson, *ACS Chem. Biol.*, 2007, **2**, 31-38.
21. Y. G. Ermakova, T. Sen, Y. A. Bogdanova, A. Y. Smirnov, N. S. Baleeva, A. I. Krylov and M. S. Baranov, *J. Phys. Chem. Lett.*, 2018, **9**, 1958-1963.
22. M.-A. Tehfe, F. Dumur, B. Graff, F. Morlet-Savary, J.-P. Fouassier, D. Gigmes and J. Lalevee, *Macromolecules*, 2013, **46**, 3761-3770.
23. H. Mokbel, F. Dumur, B. Graff, C. R. Mayer, D. Gigmes, J. Toufaily, T. Hamieh, J. P. Fouassier and J. Lalevée, *Macromol. Chem. Physics*, 2014, **215**, 783-790.
24. G. Lemercier, C. Martineau, J.-C. Mulatier, I. Wang, O. Stephan, P. Baldeck and C. Andraud, *New J. Chem.*, 2006, **30**, 1606-1613.
25. A. O. Elzoghby, W. M. Samy and N. A. Elgindy, *J. Controlled Release*, 2012, **157**, 168-182.
26. G. Kaur and O. Silakari, *Bioorg. Chem.*, 2018, **80**, 24-35.
27. M. K. Kim, H. Shin, K.-s. Park, H. Kim, J. Park, K. Kim, J. Nam, H. Choo and Y. Chong, *J. Med. Chem.*, 2015, **58**, 7596-7602.
28. B. Maji, K. Kumar, M. Kaulage, K. Muniyappa and S. Bhattacharya, *J. Med. Chem.*, 2014, **57**, 6973-6988.
29. T. L. Mistry, L. Truong, A. K. Ghosh, M. E. Johnson and S. Mehboob, *ACS Infectious Diseases*, 2017, **3**, 54-61.
30. S. Subramanian, A. Costales, T. E. Williams, B. Levine, C. M. McBride, D. Poon, P. Amiri, P. A. Renhowe, C. M. Shafer, D. Stuart, J. Verhagen and S. Ramurthy, *ACS Med. Chem. Lett.*, 2014, **5**, 989-992.
31. M.-J. Clement, K. Rathinasamy, E. Adjadj, F. Toma, P. A. Curmi and D. Panda, *Biochemistry*, 2008, **47**, 13016-13025.
32. A. Kamal, A. V. S. Rao, V. L. Nayak, N. V. S. Reddy, K. Swapna, G. Ramakrishna and M. Alvala, *Org. Biomol. Chem.*, 2014, **12**, 9864-9880.
33. D. Vela-Corcia, D. Romero, A. de Vicente and A. Perez-Garcia, *Sci. Rep.*, 2018, **8**, 1-12.
34. B. Geißel, V. Loiko, I. Klugherz, Z. Zhu, N. Wagener, O. Kurzai, C. A. M. J. J. van den Hondel and J. Wagener, *Nature Commun.*, 2018, **9**, 3098.
35. E. Horak, P. Kassal and I. Murkovic Steinberg, *Supramol. Chem.*, 2018, **30**, 838-857.
36. K. Aich, S. Das, S. Goswami, C. K. Quah, D. Sarkar, T. K. Mondal and H.-K. Fun, *New J. Chem.*, 2016, **40**, 6907-6915.
37. G. B. Bodedla, K. R. Justin Thomas, M.-S. Fan and K.-C. Ho, *J. Org. Chem.*, 2016, **81**, 640-653.
38. A. J. T. Lou, S. Righetto, C. Barger, C. Zuccaccia, E. Cariati, A. Macchioni and T. J. Marks, *J. Am. Chem. Soc.*, 2018, **140**, 8746-8755.
39. Y.-C. Wu, J.-Y. You, K. Jiang, H.-Q. Wu, J.-F. Xiong and Z.-Y. Wang, *Dyes Pigments*, 2018, **149**, 1-7.
40. A. M. Brouwer, *Pure Appl.Chem.*, 2011, **83**, 2213-2228.
41. Y. Yang, H. Xu, F. Liu, H. Wang, G. Deng, P. Si, H. Huang, S. Bo, J. Liu, L. Qiu, Z. Zhen and X. Liu, *J. Mater. Chem. C*, 2014, **2**, 5124-5132.
42. M. Paramasivam and S. Kanvah, *J. Phys.Chem. C*, 2016, **120**, 10757-10769.
43. B.-K. An, J. Gierschner and S. Y. Park, *Acc. Chem. Res.*, 2011, **45**, 544-554.

View Article Online
DOI: 10.1039/C9NJ01972C

44. G. Fan and D. Yan, *Sci. Reports*, 2014, **4**, 4933.
45. C. Reichardt, *Chem. Rev.*, 1994, **94**, 2319-2358.
46. S. Samanta, S. Halder and G. Das, *Anal. Chem.*, 2018, **90**, 7561-7568.
47. P. Singh, L. S. Mittal, S. Kaur, S. Kaur, G. Bhargava and S. Kumar, *Sensors Act. B: Chem.*, 2018, **255**, 478-489.
48. A. Divsalar, M. J. Bagheri, A. A. Saboury, H. Mansoori-Torshizi and M. Amani, *J. Phys.Chem. B*, 2009, **113**, 14035-14042.
49. Y.-Y. Wu, W.-T. Yu, T.-C. Hou, T.-K. Liu, C.-L. Huang, I. C. Chen and K.-T. Tan, *Chem. Commun.*, 2014, **50**, 11507-11510.
50. F. Kratz and B. Elsadek, *J. Contr.Release*, 2012, **161**, 429-445.
51. F. Kratz, *J. Contr. Release*, 2008, **132**, 171-183.

Graphical Abstract

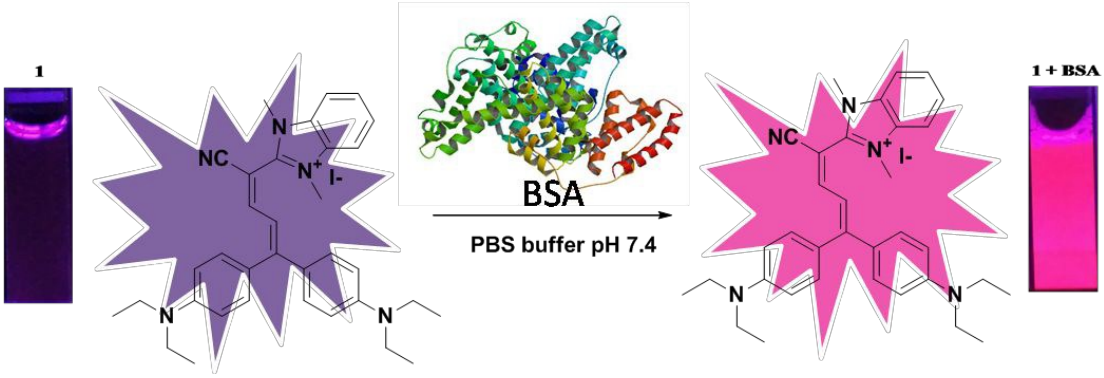

Enhanced emission and selective binding with Albumins